STATISTICS OF TURBULENCE IN BENTHAL BOUNDARY LAYERS

Ji-Fu ZHOU
Institute of Mechanics, Chinese Academy of Sciences, Beijing, 100080, China. E-mail: zhoujf@imech.ac.cn
Shu-Hui YANG
Beijing Municipal Hydraulic Research Institute, Beijing, 100044, China

Abstract: This paper deals with turbulence behavior in benthal boundary layers by means of large eddy simulation (LES). The flow is modeled by moving an infinite plate in an otherwise quiescent water with an oscillatory and a steady velocity components. The oscillatory one aims to simulate wave effect on the flow. A number of large-scale turbulence databases have been established, based on which we have obtained turbulence statistics of the boundary layers, such as Reynolds stress, turbulence intensity, skewness and flatness of turbulence, and temporal and spatial scales of turbulent bursts, etc. Particular attention is paid to the dependences of those statistics on two nondimensional parameters, namely the Reynolds number and the current-wave velocity ratio defined as the steady current velocity over the oscillatory velocity amplitude. It is found that the Reynolds stress and turbulence intensity profile differently from phase to phase, and exhibit two types of distributions in an oscillatory cycle. One is monotonic occurring during the time when current and wave-induced components are in the same direction, and the other inflectional occurring during the time when current and wave-induced components are in opposite directions. Current component makes an asymmetrical time series of Reynolds stress, as well as turbulence intensity, although the mean velocity series is symmetrical as a sine/cosine function. The skewness and flatness variations suggest that the turbulence distribution is not a normal function but approaches to a normal one with the increasing of Reynolds number and the current-wave velocity ratio as well. As for turbulent bursting, the dimensionless period and the mean area of all bursts per unit bed area tend to increase with Reynolds number and current-wave velocity ratio, rather than being constant as in steady channel flows.

Keywords: Benthal boundary layer, Turbulence, Statistics, LES, Reynolds number, Current-wave velocity ratio

1. INTRODUCTION

Turbulence behavior in a benthal boundary layer is a key issue regarding transport of nutrients, contaminants, heavy metals, and sediments, etc. in estuaries, where the flow is much different from rivers in that it cannot be assumed steady any more due to the coexistence of runoff, tides and wind waves. There have been a great number of contributions devoted to this special issue (Bonnin et al. 2006; Vittori 2003; Costamagna et al. 2003; Mellor 2002; Scotti & Piomelli 2001; Krstic & Fernando 2001; Blondeaux & Vittori 1999; Vittori & Verzicco 1998; etc.). However, owing to the complexity in this unsteady environment, previous studies have primarily focused, as Costamagna et al. (2003) pointed out, on the identification of transition between the laminar and turbulent regimes (Vittori & Verzicco 1998) and the investigation of the average characteristics (Sana & Shuy 2002; Krstic & Fernando 2001) and/or lower order statistics (i.e. Reynolds stress and turbulence intensity) of turbulence. Little attention has been devoted to higher order statistics of turbulence in this unsteady mean flow, such as skewness and flatness, which reveal the probability density distribution of turbulence. Even fewer efforts have been made to disclose the statistics of bursts in this unsteady circumstance. More and more evidences suggest close link between sediment resuspension and burst events (Bonnin et al. 2006; Vittori 2003; Nino & Garcia 1996). In particular, the temporal and spatial scales have been successfully used to parameterize sediment pickup flux in steady flows (Cao 1997). This motivates investigation of differences between bursts in steady and unsteady circumstances (Zhou 2005). With the

data obtained by means of direct numerical simulation (DNS), Costamagna et al. (2003) identified points in common and differences between wall turbulence in oscillatory boundary layers and the well-investigated turbulence structure in the steady case. Particularly, they studied the low-speed streaks and argued that a roughly reproducible mean spacing of the streaks exists in an oscillatory boundary layer and its value is close to that observed in steady boundary layers. However, the results were described only for the case of Reynolds number $\mathrm{Re}_w = \frac{u_w \delta}{\nu}$ equal to 800, where $\delta = \sqrt{2\nu/\omega}$ is the Stokes length, u_w and ω are the amplitude and the angular frequency of velocity oscillations far from the wall and ν is the kinematic viscosity of the fluid. Because of the large computational costs of DNS, the effects of Reynolds number on the statistics, especially for benthal boundary layers where currents and waves coexist, are still left open.

Thanks to large eddy simulation, which is advantageous in its compromise between accuracy and computational costs, we are able to obtain in the present paper a number of databases of different Reynolds number and current-wave velocity ratio. The Reynolds number covers a range up to 3500, for which turbulence is thought to be present throughout the whole cycle (Vittori & Verzicco 1998). The current-wave velocity ratio ranges from 0 to 3. With these databases, we have readily worked out all kinds of statistics and the characteristics of bursts in the benthal boundary layers. Furthermore, we have investigated the effects of Reynolds number and current-wave velocity ratio on the statistics.

2. LES OF BENTHAL BOUNDARY LAYERS

To make a compromise between computational costs and turbulence-resolution, we hereby conduct large eddy simulations (LES) for benthal boundary layers. The flow is simulated by moving a plate in a quiescent water with a periodic velocity component $u_w \cos(\omega t)$, superimposed by a steady speed component u_c. If the reference frame is fixed on the plate, the boundary layer is exactly that induced by a steady current of velocity u_c and a surface wave with its resultant sea bottom velocity of $u_w \cos(\omega t)$.

The filtered 3-D Navier-Stokes equations for incompressible fluids are adopted. The subgrid stress is calculated by Smargrinsky model (Smargrinsky 1963) revised with Van Driest damping function. A certain number of nonuniform grids are used in the wall-normal direction to resolve the fine structure in the near-wall region (Zhou 2005; Zhang 2005).

The boundary layer behavior depends substantially on two dimensionless parameters, namely the Reynolds number Re_w as already defined in the introduction and the current-wave velocity ratio u_c/u_w. If $u_c/u_w \gg 1$, the flow behaves like a steady boundary layer of channel flows. If $u_c/u_w \ll 1$, the flow approaches to a pure oscillatory boundary layer.

Previous studies (Vittori & Verzicco 1998; Jensen et al. 1989) have identified four regimes of a pure oscillatory boundary layer: the laminar regime ($\mathrm{Re}_w < 100$), the disturbed laminar regime ($100 < \mathrm{Re}_w < 500$), the intermittently turbulent regime ($500 < \mathrm{Re}_w < 3500$) and the fully turbulent regime ($\mathrm{Re}_w > 3500$). To manifest the effects of Reynolds number on turbulence behavior, we have here simulated several cases with Reynolds number covering the range from 1000 to 3500. In the meantime, current component is simultaneously modeled with the current-wave velocity ratio ranged from 0 to 3. The case with the current-wave velocity ratio equal to 0 represents a purely wave-induced flow.

3. RESULTS AND DISCUSSIONS

3.1 Reynolds Stress and Turbulence Intensity

Here, we mean by "Reynolds stress" the large-scale Reynolds stress, i.e. $<-u''w'>$, where u'' and w' respectively stand for the large-scale streamwise and wall-normal fluctuations, and $<\bullet>$ performs time average of plane-averaged quantities.

Fig. 1 shows the Reynolds stress profiles at phases of every $\pi/6$ of the cycle for the cases of different current-wave velocity ratios with an identical Reynolds number of 1000. From this figure, the following are observed.

- There exist two types of Reynolds stress profiles, one being monotonic and the other inflectional. When the phase falls into the interval [0, $\pi/2$] or [$3\pi/2$, 2π], the Reynolds stress profile is a monotonic curve with its peak value near the wall, which behaves like that of unidirectional channel flows. This is simply because the current component is along with the wave-induced velocity near the wall during this phase range. On the other hand, the current component goes against the wave-induced velocity near the wall when the phase falls into the range [$\pi/2$, $3\pi/2$]. This fact leads to a inflectional Reynolds stress profile with an inflexion at a certain distance from the wall. The peak Reynolds stress seems to locate in a range of $10 < z/\delta < 50$, further from the wall than in pure wave boundary layers where the peak Reynolds stress is below $z/\delta = 15$.
- The location of the inflexion of the second type of Reynolds stress profile varies with phase and current-wave velocity ratio as well. After its birth at the phase of $\pi/2$, it gradually moves upwards from the near-bed vicinity till about $z/\delta = 50$ at the phase of $3\pi/2$. Then, the inflexion disappears and the profile turns to a monotonic one. At a given phase, the inflexion locates at a higher position for a higher current-wave velocity ratio.
- The Reynolds stress increases with the current-wave velocity ratio at all phases.
- The peak Reynolds stress occurs at the phase when current and wave-induced velocity components are in the same direction.

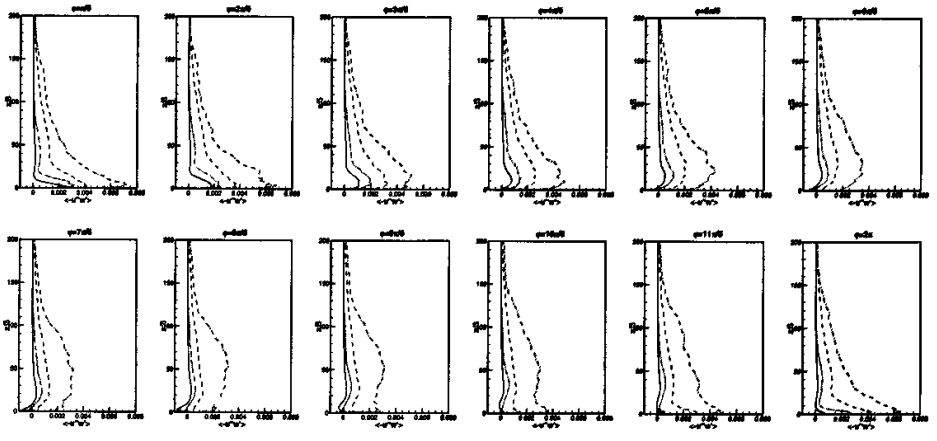

Fig. 1 Vertical distribution of Reynolds stress at different phases of the cycle ($Re_w = 1000$). Solid, dot-dot-dashed, dashed and dot-dashed lines respectively corresponds to $u_c/u_w = 0.5, 1.0, 2.0, 3.0$. u'' and w' are the large-scale streamwise and wall-normal fluctuations. z is the wall-normal coordinate.

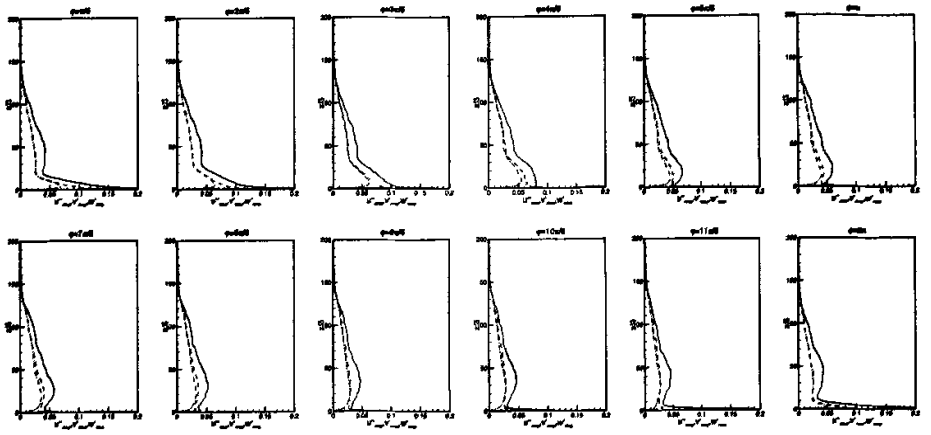

Fig. 2 Vertical distribution of turbulence intensity at different phases of the cycle (for $\mathrm{Re}_w = 1000$ and $u_c / u_w = 1.0$). u''_{rms} (solid line), v'_{rms} (dashed line) and w'_{rms} (dot-dashed line) respectively represent the root-mean-squares of large-scale streamwise, spanwise and wall-normal fluctuations.

Fig. 2 illustrates vertical distribution of turbulence intensity at phases of every $\pi/6$ of the cycle for $\mathrm{Re}_w = 1000$ and $u_c / u_w = 1.0$, in which u''_{rms}, v'_{rms}, w'_{rms} represent the root-mean-squares of large-scale streamwise, spanwise and wall-normal velocity fluctuations, respectively. It is seen that: if the phase is in the interval [0, $\pi/2$] or [$3\pi/2$, 2π] when current and wave-induced velocity components are in the same direction, the turbulence intensity profile is basically monotonic with its peak value near the wall; otherwise, if the phase is in the interval [$\pi/2$, $3\pi/2$] when current and wave-induced velocity components are in opposite directions, the turbulence intensity profile turns to be non-monotonic and its peak value locates at a certain distance away from the wall. It is also noted that the peak turbulence intensity of the cycle occurs at the phase when current and wave-induced velocity components are in the same direction.

3.2 Skewness and Flatness of Turbulence

Skewness and flatness of turbulence are respectively three- and four-order moments of velocity fluctuations. The former accounts for the symmetry of velocity distribution about its expectation, while the latter describes the flatness of the probability density distribution curve. For a normal distribution, the skewness is zero and the flatness 3. A larger flatness implies stronger turbulence intermittency.

Fig. 3 illustrates the skewness [Fig. 3(a)] and flatness [Fig. 3 (b)] profiles of the streamwise velocity fluctuations corresponding to different current-wave velocity ratios with an identical Reynolds number. Fig. 4 shows the skewness [Fig. 4 (a)] and flatness [Fig. 4 (b)] profiles of the streamwise velocity fluctuations corresponding to different Reynolds numbers with an identical current-wave velocity ratio. It is noted from Fig. 3 and Fig. 4 that both the skewness and flatness vary with the two governing dimensionless parameters. The larger the Reynolds number or the current-wave velocity ratio, the closer to 0 the skewness and the closer to 3 the flatness. This implies that the probability distribution of the streamwise velocity fluctuations approaches to the normal distribution with the increasing of Reynolds number and the current-wave velocity ratio as well. In addition, it is apparently seen that the effects of the two dimensionless parameters on the probability distribution of the streamwise fluctuations are more evident in the near wall region, say z/δ<30.

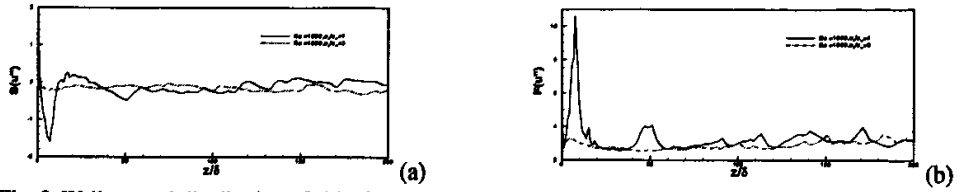

Fig. 3 Wall-normal distribution of (a) skewness and (b) flatness of streamwise fluctuations for different current-wave velocity ratio with an identical Reynolds number.

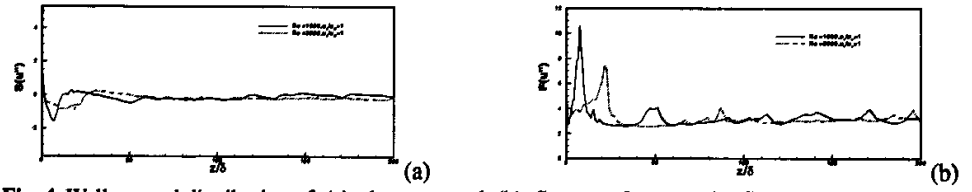

Fig. 4 Wall-normal distribution of (a) skewness and (b) flatness of streamwise fluctuations for different Reynolds number with an identical current-wave velocity ratio.

3.3 Turbulent Bursting Characteristics

Bursting is a coherent structure in turbulent flows. It is a key mechanism for sediment incipience (Nino & Garcia 1996). The characteristics of the bursts, such as the period and the scales of the low-speed streaks, in steady channel flows have been well investigated (Robinson 1991). And the dimensionless bursting period T^+ and the mean area of all bursts per unit bed area λ were successfully used to parameterize sediment entrainment flux in steady channel flows (Cao 1997). As far as sediment transport in unsteady coastal flows is concerned, it is now necessary to manifest the two parameters, T^+ and λ, in benthal boundary layers.

Based on the large-scale turbulence databases obtained by LES, we may readily extract the dimensionless bursting period and the mean area of all bursts per unit bed area by means of wavelet analysis and quadrant 2 conditional sampling, respectively. Fig. 5 displays the dependence of the dimensionless bursting period on Re_w and u_c/u_w. It is seen that T^+ increases with both Re_w and u_c/u_w. This is different from that in steady channel flows, where the dimensionless bursting period is roughly a constant, independent of Reynolds number. Fig. 6 depicts λ against threshold for different values of Re_w and u_c/u_w. It is apparent that λ also increases with both Re_w and u_c/u_w at a given threshold.

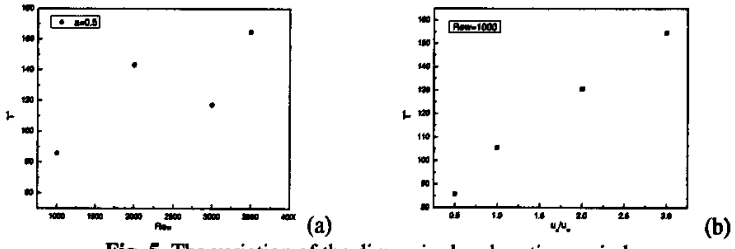

Fig. 5 The variation of the dimensionless bursting period with (a) Reynolds number and (b) current-wave velocity ratio.

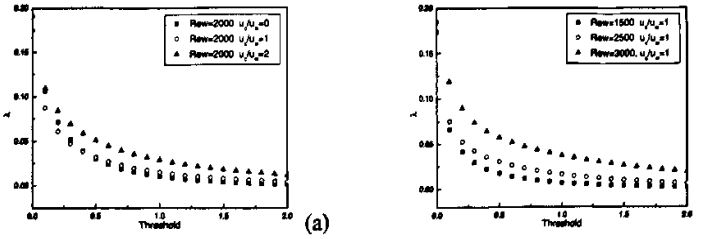

(a) (b)

Fig. 6 The variation of the mean area of all bursts per unit bed area with (a) Reynolds number and (b) current-wave velocity ratio.

4. CONCLUSIONS

In the present paper, we have conducted large eddy simulation for benthal boundary layers, obtaining a number of large-scale turbulence databases. Based on these databases, statistics of turbulence in benthal boundary layers are readily acquired. The following conclusions are obtained.

- There seems to exist two types of Reynolds stress profiles and turbulence intensity profiles as well. The first one is monotonic with its peak value near the wall and the second one is inflectional with its peak value at a certain distance from the wall. The monotonic profiles occur during the time when current and wave-induced velocity components are in the same direction, while the inflectional ones occur during the time when current and wave-induced velocity components are in opposite directions.
- Both Reynolds stress and turbulence intensity increase with Reynolds number and current-wave velocity ratio at any phases.
- The peak values of Reynolds stress and turbulence intensity in an oscillatory cycle occur at the phase when current and wave-induced velocity components are in the same direction.
- The skewness and flatness of streamwise turbulence in benthal boundary layers fluctuate, respectively, around 0 and 3. And the fluctuations tend to diminish, especially in the near wall region, with the increasing of Reynolds number and/or current-wave velocity ratio. This implies that the probability distribution of the streamwise turbulence approaches to the normal distribution with the increasing of Reynolds number and the current-wave velocity ratio as well.
- Unlike in steady channel flows, both the dimensionless bursting period and the mean area of all bursts per unit bed area in benthal boundary layers increase with Reynolds number and/or current-wave velocity ratio.

ACKNOWLEDGMENT

We would like to give thanks to the financial support from the National Natural Science Foundation of China under Grant Nos. 10572144 and 10332050. We also appreciate the support of the Innovation Project of Chinese Academy of Sciences under the grant No. KJCX-SW-L08.

REFERENCES

Blondeaux, P. & Vittori, G. 1999, Boundary layer and sediment dynamics under sea waves. Adv. Coast. Ocean Engng., 4, 133-190.

Bonnin J, Van Haren H, Hosegood P, Brummer GJA, 2006, Burst resuspension of seabed material at the foot of the continental slope in the Rockall Channel. MARINE GEOLOGY, 226 (3-4): 167-184.

Cao ZX, 1997, Turbulent bursting-based sediment entrainment function. J. Hydr. Engrg., 123(3): 233-236.

Costamagna P, Vittori G, Blondeaux P, 2003, Coherent structures in oscillatory boundary layers. JOURNAL OF FLUID MECHANICS, 474: 1-33.

Jensen BL, Sumer BM & Fredsoe, J, 1989, Turbulent oscillatory boundary layers at high Reynolds numbers. JOURNAL OF FLUID MECHANICS, 206: 256-297.

Ji-Fu Zhou, Jia-Chun Li. 2005, Modeling storm-induced current circulation and sediment transport in a schematic harbor. Journal of Waterway, Port, Coastal and Ocean Engineering, 131(1): 25-32

Krstic RV, Fernando HJS, 2001, The nature of rough-wall oscillatory boundary layers. JOURNAL OF HYDRAULIC RESEARCH, 39 (6): 655-666.

Nezu, Iehisa and Sanjou, Michio, 2006, Numerical calculation of turbulence structure in depth-varying unsteady open-channel flows. Journal of Hydraulic Engineering, 132(7): 681 – 695

Nino Y and Garcia MH, 1996, Experiments on Particle-Turbulence Interactions in the Near-Wall Region of an Open Channel Flow: Implications for Sediment Transport. J. Fluid Mech., 326, 285-319.

Robinson, S. K. 1991 Coherent motions in the turbulent boundary layer. Annu. Rev. Fluid Mech., 23, 601-639.

Sana A, Shuy EB, 2002, Two-equation turbulence models for smooth oscillatory boundary layers. JOURNAL OF WATERWAY PORT COASTAL AND OCEAN ENGINEERING, 128 (1): 38-45.

Scotti A, Piomelli U, 2001, Numerical simulation of pulsating turbulent channel flow. PHYSICS OF FLUIDS, 13 (5): 1367-1384.

Smagorinsky J. 1963, General circulation experiments with the prinitive equations, I. The basic experiment [J]. Mon Weather Rev, 91:99-164.

Vittori G, 2003, Sediment suspension due to waves. JOURNAL OF GEOPHYSICAL RESEARCH-OCEANS, 108 (C6): 3173-.

Vittori, G. & Verzicco, R. 1998, Direct simulation of transition in an oscillatory boundary layer. J. Fluid Mech., 371, 207-232.

ZHANG Qiang, ZHOU Jifu & LI Jiachun, 2005, Burst detection in turbulent channel flows based on large eddy simulation databases. Science in China Ser. G Physics, Mechanics & Astronomy, 48(4): 469-484.

Zhou Ji-Fu, Zhang Qiang, Li Jia-Chun. 2005, Probability distribution function of near-wall turbulent velocity fluctuations. Applied Mathematics and Mechanics, 26(10): 1245-1254.